



# LUND UNIVERSITY

## Direct measurement of S-branch N(2)-H(2) Raman linewidths using time-resolved pure rotational coherent anti-Stokes Raman spectroscopy.

Bohlin, Alexis; Nordström, Emil; Patterson, B D; Bengtsson, Per-Erik; Kliewer, C J

*Published in:*  
Journal of Chemical Physics

*DOI:*  
[10.1063/1.4742915](https://doi.org/10.1063/1.4742915)

2012

[Link to publication](#)

*Citation for published version (APA):*  
Bohlin, A., Nordström, E., Patterson, B. D., Bengtsson, P.-E., & Kliewer, C. J. (2012). Direct measurement of S-branch N(2)-H(2) Raman linewidths using time-resolved pure rotational coherent anti-Stokes Raman spectroscopy. *Journal of Chemical Physics*, 137(7), Article 074302. <https://doi.org/10.1063/1.4742915>

*Total number of authors:*  
5

### General rights

Unless other specific re-use rights are stated the following general rights apply:  
Copyright and moral rights for the publications made accessible in the public portal are retained by the authors and/or other copyright owners and it is a condition of accessing publications that users recognise and abide by the legal requirements associated with these rights.

- Users may download and print one copy of any publication from the public portal for the purpose of private study or research.
- You may not further distribute the material or use it for any profit-making activity or commercial gain
- You may freely distribute the URL identifying the publication in the public portal

Read more about Creative commons licenses: <https://creativecommons.org/licenses/>

### Take down policy

If you believe that this document breaches copyright please contact us providing details, and we will remove access to the work immediately and investigate your claim.

LUND UNIVERSITY

PO Box 117  
221 00 Lund  
+46 46-222 00 00

## Direct measurement of S-branch N<sub>2</sub>-H<sub>2</sub> Raman linewidths using time-resolved pure rotational coherent anti-Stokes Raman spectroscopy

A. Bohlin, E. Nordström, B. D. Patterson, P.-E. Bengtsson, and C. J. Kliewer

Citation: *J. Chem. Phys.* **137**, 074302 (2012); doi: 10.1063/1.4742915

View online: <http://dx.doi.org/10.1063/1.4742915>

View Table of Contents: <http://jcp.aip.org/resource/1/JCPSA6/v137/i7>

Published by the [American Institute of Physics](#).

---

### Additional information on *J. Chem. Phys.*


Journal Homepage: <http://jcp.aip.org/>

Journal Information: [http://jcp.aip.org/about/about\\_the\\_journal](http://jcp.aip.org/about/about_the_journal)

Top downloads: [http://jcp.aip.org/features/most\\_downloaded](http://jcp.aip.org/features/most_downloaded)

Information for Authors: <http://jcp.aip.org/authors>

## ADVERTISEMENT



**AIPAdvances**

Special Topic Section:  
**PHYSICS OF CANCER**

Why cancer? Why physics? [View Articles Now](#)

# Direct measurement of S-branch N<sub>2</sub>-H<sub>2</sub> Raman linewidths using time-resolved pure rotational coherent anti-Stokes Raman spectroscopy

A. Bohlin,<sup>1</sup> E. Nordström,<sup>1</sup> B. D. Patterson,<sup>2</sup> P.-E. Bengtsson,<sup>1</sup> and C. J. Kliwer<sup>2</sup>

<sup>1</sup>*Division of Combustion Physics, Lund University, P.O. Box 118, 221 00 Lund, Sweden*

<sup>2</sup>*Combustion Research Facility, Sandia National Laboratory, P.O. Box 969 MS 9055, Livermore, California 94551, USA*

(Received 30 March 2012; accepted 23 July 2012; published online 15 August 2012)

S-branch N<sub>2</sub>-H<sub>2</sub> Raman linewidths have been measured in the temperature region 294–1466 K using time-resolved dual-broadband picosecond pure rotational coherent anti-Stokes Raman spectroscopy (RCARS). Data are extracted by mapping the dephasing rates of the CARS signal temporal decay. The *J*-dependent coherence decays are detected in the time domain by following the individual spectral lines as a function of probe delay. The linewidth data set was employed in spectral fits of N<sub>2</sub> RCARS spectra recorded in binary mixtures of N<sub>2</sub> and H<sub>2</sub> at calibrated temperature conditions up to 661 K using a standard nanosecond RCARS setup. In this region, the set shows a deviation of less than 2% in comparison with thermocouples. The results provide useful knowledge for the applicability of N<sub>2</sub> CARS thermometry on the fuel-side of H<sub>2</sub> diffusion flames. © 2012 American Institute of Physics. [<http://dx.doi.org/10.1063/1.4742915>]

## I. INTRODUCTION

Pure rotational coherent anti-Stokes Raman spectroscopy (RCARS) has been developed over the last decades to become a frequent tool for non-intrusive temperature measurements in combustion.<sup>1,2</sup> In air-fed flames, RCARS thermometry has been achieved mainly with N<sub>2</sub> as the probed molecule because of its high abundance and inert properties. When probing rotational N<sub>2</sub> S-branch transitions, the highest sensitivity is obtained in the low-temperature regime, which makes the technique well suited for studies of pre-combustion conditions. One specific example is the fuel-side of diffusion flames, where the heating of the fuel can be studied before ignition. However, for CARS to be successfully applied in environments where the gas mixture composition is dominated by fuel species, an accurate linewidth model must be employed, which takes account of collisional broadening of the N<sub>2</sub> Raman lines by fuels, and there is currently a lack of literature for most N<sub>2</sub>-fuel collision partners.

In a previous investigation where N<sub>2</sub> RCARS thermometry was applied on the fuel-side of a H<sub>2</sub>/air-diffusion flame,<sup>3</sup> the accuracy obtained was very much dependent on employing an adequate Raman linewidth model. This linewidth model employed needs to simulate the effects from molecular collisions on the frequency-resolved N<sub>2</sub> spectral lines inquired with a nanosecond temporal probe pulse. It is well known that to assess accurate temperatures with RCARS, the broadening from all major collision partners needs to be incorporated.<sup>4</sup> There are some colliders that are more critical than others for accurate thermometry, which is related to the specific *J*-dependence of the broadening coefficients. One such critical species is H<sub>2</sub>, and in a combined experimental and theoretical effort, N<sub>2</sub>-H<sub>2</sub> line-broadening coefficients have been published previously.<sup>5–7</sup> When including these Raman linewidths<sup>7</sup> in evaluations of N<sub>2</sub> RCARS spec-

tra, recorded in the product gases of a rich hydrocarbon flame containing 20% H<sub>2</sub>, the predicted temperature was systematically increased by about 2%.<sup>8</sup> This behavior was confirmed in a subsequent study, probing N<sub>2</sub> in binary mixtures with H<sub>2</sub> at calibrated temperature conditions below 800 K.<sup>9</sup> Here, it was shown that when neglecting the effects on the N<sub>2</sub> spectral lines in the environment dominated by collisions with H<sub>2</sub>, predicted temperatures from N<sub>2</sub> RCARS could be underestimated by as much as 6%–7%. However, by modifying the Raman linewidth model to incorporate each of the species-specific contributions to the broadening coefficient, weighted in accordance with their relative mole fractions, the thermometry was improved. Still, a slight thermometric overestimation remained, which has motivated a continuation of that study, and is accordingly the subject of this article.

The discrepancy in thermometry observed in Bohlin *et al.*<sup>9</sup> may be related to a minor inaccuracy in the *J*-dependence of the employed N<sub>2</sub>-H<sub>2</sub> coefficients. Through a previous benchmark in the field, these were derived by fitting an energy-corrected sudden exponential-polynomial (ECS-EP) dynamical scaling law<sup>10,11</sup> to experimental data obtained with high-resolution stimulated Raman loss spectroscopy.<sup>5</sup> However, the vulnerability of such a procedure is the reliance on extrapolation, where the predictions have not been well studied experimentally. The validity of the extrapolated N<sub>2</sub>-H<sub>2</sub> ECS-EP values was also debated in a recent publication,<sup>12</sup> where a comparison with close-coupling and couple-states quantum dynamical calculations up to 2000 K indicated an underestimation of about 20% in the results of the scaling law. Capturing the collisional dynamics in an extensive range of both temperature as well as rotational quantum number is the focus of this study. To this end, we apply a recent experimental development enabling direct measurement of Raman broadening coefficients using time-resolved picosecond RCARS.

Picosecond RCARS<sup>13–16</sup> has been developed in the past few years to become a candidate for gas-phase thermometry with the same capability as a standardized nanosecond setup. However, with the added ability of delaying the probe pulse beyond the temporal envelope of the time-coincident pump and Stokes pulses, this approach has the advantage to be able to circumvent some of the difficulties connected to experiments in the nanosecond regime, such as the non-resonant background<sup>13</sup> and smeared vibrational CARS signals.<sup>14</sup> The same ability together with the high peak-power of picosecond laser pulses allows for rapid determination of accurate Raman linewidths up to elevated temperatures relevant for flame studies, and for each temperature the technique may provide a complete set of  $J$ -specific line-broadening coefficients. The method is based on monitoring the  $J$ -dependent CARS signal decay as a function of probe delay such that the collisional dephasing of each of the Raman coherences is detected in the time domain. At atmospheric pressure, RCARS from  $N_2$  is well within the pressure limit of the isolated line approximation.<sup>17</sup> Thus, the Raman Lorentzian linewidth (full width at half maximum, FWHM) is given by

$$\Gamma_{J''} = (2\pi c \tau_{\text{CARS}, J''})^{-1}, \quad (1)$$

where  $c$  is the speed of light (cm/s),  $\tau_{\text{CARS}, J''}$  is the exponential decay time constant for the coherence decay (s), and  $\Gamma_{J''}$  is the Raman linewidth (FWHM,  $\text{cm}^{-1}$ ). Such measurements were performed in connection to the current study, reporting self-broadened S-branch  $N_2$ - $N_2$  Raman linewidths in the temperature range 294–1466 K.<sup>18</sup> In Ref. 18, comparisons were made to the ECS (Ref. 19) and modified exponential gap<sup>20</sup> dynamical scaling laws, and the results were used to quantify the sensitivity of nanosecond RCARS thermometry to the linewidth model employed. The overall uncertainty based on the linewidth model used in pure  $N_2$  was estimated to be 2%. Nanosecond RCARS spectra were recorded in 100%  $N_2$  in a temperature calibrated cell at up to 800 K, and by implementing the  $N_2$ - $N_2$  time-domain coefficients in the spectral library simulated to fit the spectra, the evaluated temperatures deviated by less than 1% from the reference temperature.

In this study, we utilize the same method in deriving S-branch  $N_2$  Raman linewidths as a function of temperature where  $N_2$  is perturbed by a foreign collider. Results of experimentally measured S-branch  $N_2$ - $H_2$  line-broadening coefficients are reported in the temperature range 294–1466 K at pressure of 1 atm. The obtained time-domain coefficients are then tested for RCARS thermometry by being employed in spectral fits of  $N_2$  spectra recorded in binary mixtures with  $H_2$  at calibrated oven temperatures up to 661 K. The conditions are applied to mimic the fuel-side of  $H_2$ /air diffusion flames.

## II. TIME-DOMAIN MEASUREMENTS

The picosecond RCARS experimental apparatus used in this study has been described in a study made in connection to these experiments<sup>18</sup> and is only briefly outlined here. The pump and Stokes pulses were produced with a 20-Hz regeneratively amplified mode-locked Nd:YAG laser pumping a broadband dye laser, which consisted of an amplified spontaneous emission (ASE) source fol-

lowed by two amplification stages prepared with an ethanol dye solution of DCM (4-(dicyanomethylene)-2-methyl-6-(4-dimethylaminostyryl)-4*H*-pyran) centered at 633 nm. The pulse widths were approximately 100 ps. A polarizing beam splitter was used to split the 633-nm beam into equal pump and Stokes beams, and a mechanical delay stage was placed in the Stokes beam path to zero the delay between pump and Stokes at initial setup. A second regeneratively amplified Nd:YAG laser provided the narrowband probe beam at 532 nm. Both lasers were locked to the same RF source, allowing precise electronic timing of the probe pulse with respect to the pump and Stokes pulses from  $-200$  ps to  $+1$  ns in 20-ps time-steps. The RCARS probe volume was formed using a planar BOXCARS geometry with a 500-mm focal length lens. To spectrally filter the CARS beam from interfering light, the signal was directed through several dichroic mirrors and short-pass filters along the detection path. A 100-mm focal length spherical lens was used to focus the signal onto a 1-m spectrometer equipped with an 1800-line/mm grating to disperse the RCARS signal. The signal was detected using a back-illuminated CCD camera (Andor Newton), and having a pixel size of  $16 \mu\text{m}$  the spectra were recorded with a dispersion of  $0.29 \text{ cm}^{-1}/\text{pixel}$ . A temperature-controlled oven was filled with  $N_2$  in binary mixtures of 0%, 50%, and 80%  $H_2$  at temperatures ranging from 295 K to 1466 K. For each temperature, spectra were recorded for a series of approximately 30 probe delays. At each probe delay, 20 laser shots were accumulated on the CCD per readout, and a series of 40 readouts were individually saved. In accordance with standard post-processing, the spectra were subtracted with a recorded background and divided with a non-resonant spectrum recorded in argon in order to spectrally compensate for the finite width of the broadband emission profile and the transmission characteristics along the detection path.

By monitoring the RCARS spectrum as a function of probe delay, as shown in Fig. 1, the  $J$ -specific exponential

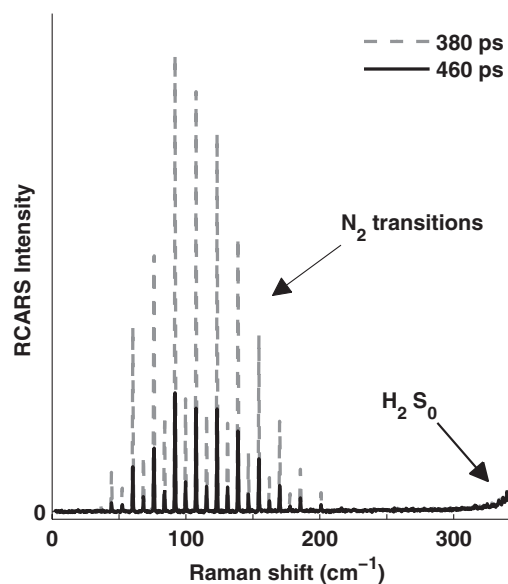


FIG. 1. RCARS spectra recorded at 395 K in a mixture of  $H_2$  and  $N_2$  (80%  $H_2$ /20%  $N_2$ ) for probe delays of 380 and 460 ps. The Lorentzian wing of the  $H_2$   $S_0$  transition is noted.

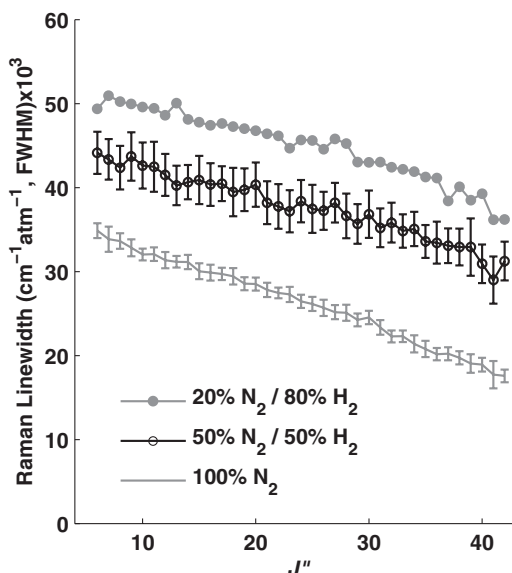


FIG. 2. Measured time-domain S-branch Raman linewidths for  $N_2$  with various  $H_2$  concentrations at 1466 K. The error bars represent the  $\pm 2\sigma$  uncertainty in the measurement.

decay constants,  $\tau_{\text{CARS}, J''}$  were determined by an exponential fit to the decay of signal under each  $J$ -line and used to calculate the frequency-domain Raman linewidth  $\Gamma_{J''}$  according to Eq. (1).

In order to extract the  $J$ -dependent and temperature-dependent  $N_2$ - $H_2$  broadening coefficient, measurements were recorded in mixtures of  $N_2$  and  $H_2$  for each temperature. Measurements were made at 20%, 50%, and 100%  $N_2$  concentrations. A simple linear extrapolation was made from the 100% and 50%  $N_2$  mixtures to determine the measured  $N_2$ - $H_2$  broadening coefficient. One validation of the linear extrapolation was the agreement with the measured Raman linewidths for the 20%  $N_2$  mixture. Figure 2 displays the measured  $N_2$  Raman linewidths at 1466 K in the three different  $N_2$  concentrations and the error bars represent the  $\pm 2\sigma$  uncertainty.

For the pure  $N_2$  measurements, the uncertainty in the resulting calculated Raman linewidth was less than in the 50% and 20%  $N_2$  case because of the lower  $N_2$  signals in these cases. Whereas the  $2\sigma$  uncertainty in pure  $N_2$  was typically 2%–3% of the Raman linewidth, the uncertainty was typically 5%–6% in the case of the 20% and 50%  $N_2$  (balance  $H_2$ ) mixtures. These errors propagated to the resulting temperature-dependent  $N_2$ - $H_2$  broadening coefficient result in a total  $2\sigma$  uncertainty of about 6% or less.

The extracted time-domain  $N_2$ - $H_2$  (closed black circles) and  $N_2$ - $N_2$  (Ref. 18) (open black circles) S-branch Raman linewidths are presented in Fig. 3.

The measurements were performed at temperatures 294 K, 395 K, 495 K, 661 K, 868 K, 1116 K, and 1466 K. The linewidths generally decrease with temperature, as seen in Fig. 3, where the line-broadening coefficients are expressed as  $\text{cm}^{-1}/\text{atm}$  at full width at half maximum. It should be noticed that the experimental uncertainties of the measured  $N_2$ - $H_2$  coefficients are slightly increased in comparison with the self-broadened  $N_2$ - $N_2$  coefficients,<sup>18</sup> since in the binary mixtures with equal amount of  $H_2$  or more, the recording of the

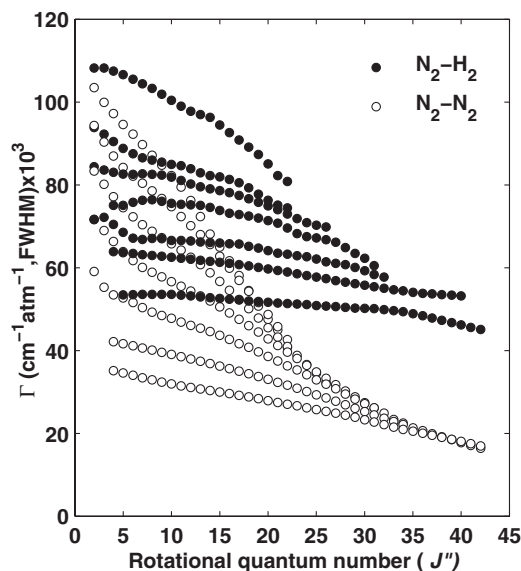


FIG. 3. Measured time-domain S-branch Raman linewidths for  $N_2$ - $H_2$  (closed black circles) and  $N_2$ - $N_2$ <sup>18</sup> (open black circles) at temperatures 294 K, 395 K, 495 K, 661 K, 868 K, 1116 K, and 1466 K.

$N_2$ -lines gets affected by reduced signal levels. The RCARS signal has a square dependence on the number density and in addition the dephasing of the  $N_2$  coherences gets increased in the presence of  $H_2$ . The comparison with self-broadened coefficients is also made to illustrate the very different  $J$ -dependencies of these two systems. In a simplified description, the rotational energy transfer between an initial and the final state is suppressed by a discrepancy in energy or angular momenta between the states. In the autoperturbative mixture, the rotational energy of the active molecule ( $N_2$ ) can be transferred more easily to neighboring states of the perturber ( $N_2$ ); the transfer of rotational energy from the lower  $J$  states of the active molecule is more probable than it is from the higher  $J$  states (according to the thermal population distribution of the energy levels). This is the reason for the decrease in  $N_2$ - $N_2$  Raman linewidths being a function of the rotational state involved ( $J$ -dependence). In contrast, for collisions with a foreign molecule  $H_2$ , there is a discrepancy in neighboring states between the perturber and the active  $N_2$  for each of the  $J$  states. This makes the  $J$ -dependence of the  $N_2$ - $H_2$  Raman linewidths becoming less pronounced. The smooth variation of the  $N_2$ - $H_2$  coefficients is an effect of a considerable large spacing between the rotational energy levels of  $H_2$ ; that is why the  $N_2$  molecules regardless of  $J$  state have difficulties in transferring rotational energy to  $H_2$ . When  $N_2$  collides (inelastically) with  $H_2$ , the  $H_2$  molecule changes its speed rather than its rotation. The considerable level in absolute broadening of the  $N_2$ - $H_2$  collision is an effect of the relatively larger speed from a lightweight molecule, such as  $H_2$ , reaching closer to the repulsive wall of the  $N_2$  interaction potential. This pronounced difference in  $J$ -dependence of these colliding systems is the reason for systematic errors in RCARS thermometry if neglecting to incorporate the  $N_2$ - $H_2$  Raman linewidths in environments where a significant fraction of the  $N_2$ -collisions are with  $H_2$ .



TABLE I. S-branch N<sub>2</sub>-H<sub>2</sub> Raman linewidths (cm<sup>-1</sup> atm<sup>-1</sup>, FWHM).

$J''$	294 K	395 K	495 K	661 K	868 K	1116 K	1466 K
2	0.108	0.094	0.084	...	0.072	...	...
3	0.108	0.092	0.084	...	0.072	...	...
4	0.107	0.090	0.083	0.075	0.070	0.064	...
5	0.107	0.089	0.083	0.075	0.069	0.064	0.053
6	0.105	0.088	0.083	0.076	0.067	0.063	0.053
7	0.104	0.087	0.083	0.076	0.067	0.063	0.054
8	0.103	0.086	0.083	0.076	0.067	0.063	0.054
9	0.102	0.086	0.082	0.076	0.067	0.063	0.054
10	0.100	0.085	0.082	0.076	0.067	0.063	0.054
11	0.099	0.085	0.081	0.075	0.067	0.062	0.053
12	0.098	0.084	0.080	0.075	0.066	0.062	0.053
13	0.097	0.083	0.080	0.075	0.066	0.062	0.053
14	0.096	0.082	0.079	0.075	0.066	0.062	0.053
15	0.094	0.082	0.079	0.074	0.066	0.061	0.053
16	0.092	0.081	0.078	0.073	0.066	0.061	0.052
17	0.091	0.081	0.077	0.073	0.066	0.061	0.052
18	0.089	0.079	0.077	0.072	0.065	0.060	0.052
19	0.087	0.078	0.076	0.072	0.065	0.060	0.052
20	0.085	0.076	0.075	0.071	0.064	0.060	0.052
21	0.082	0.075	0.074	0.071	0.063	0.059	0.052
22	0.081	0.074	0.073	0.070	0.063	0.059	0.051
23	...	...	0.072	0.068	0.063	0.059	0.051
24	...	...	0.071	0.067	0.063	0.058	0.051
25	...	...	0.070	0.067	0.062	0.058	0.051
26	...	...	0.070	0.067	0.061	0.057	0.051
27	...	...	...	0.066	0.061	0.057	0.051
28	...	...	...	0.065	0.061	0.057	0.050
29	...	...	...	0.063	0.060	0.056	0.050
30	...	...	...	0.062	0.059	0.056	0.050
31	...	...	...	0.061	0.058	0.055	0.050
32	...	...	...	...	0.058	0.055	0.050
33	...	...	...	...	...	0.055	0.050
34	...	...	...	...	...	0.054	0.049
35	...	...	...	...	...	0.054	0.049
36	...	...	...	...	...	0.054	0.048
37	...	...	...	...	...	0.054	0.048
38	...	...	...	...	...	0.054	0.047
39	...	...	...	...	...	0.053	0.047
40	...	...	...	...	...	0.053	0.046
41	...	...	...	...	...	...	0.046
42	...	...	...	...	...	...	0.045

Further, the unique capability of the technique to measure line-broadening coefficients *in situ* in an extended range of both temperatures and rotational quantum number is demonstrated. It is estimated that the range of  $J$ -coefficients in the presented data covers more than 95% of the total N<sub>2</sub> thermal population distribution at the measured temperatures, which avoids the necessity of extrapolation that might hazard the accuracy of RCARS thermometry. In order to serve the CARS community with a useful data set, the derived S-branch N<sub>2</sub>-H<sub>2</sub> Raman linewidths are given in Table I.

### III. IMPLEMENTATION FOR RCARS THERMOMETRY

To validate the N<sub>2</sub>-H<sub>2</sub> coefficients obtained from measurements in the time domain, they were employed in fitting nanosecond RCARS spectra recorded at binary mixtures of N<sub>2</sub> and H<sub>2</sub> in a set of calibrated heated cell ex-

periments. These validation experiments were performed by the same procedure and experimental setup as described in Ref. 9. The thermometry is based on a standard contour spectral fitting procedure, where the experimental spectrum is compared with a library of pre-calculated theoretical spectra at different temperatures of the prevailing experimental conditions. The routine is built on a nonlinear interpolating Levenberg-Marquardt algorithm to minimize the sum square of the residuals (SSQ) between experimental and theoretical spectra. The theoretical spectra were calculated using an in-house-developed RCARS code,<sup>21</sup> updated with more recent N<sub>2</sub> Herman-Wallis factors,<sup>22,23</sup> to improve the accuracy in evaluated data. In Ref. 9, the theoretical spectra were composed with N<sub>2</sub> spectral lines only, motivated by an insignificant spectral interference between the two species, N<sub>2</sub> and H<sub>2</sub>, which are well separable in frequency. At temperatures below 800 K, the N<sub>2</sub> spectral envelope covers a region of about 250 wavenumbers (cm<sup>-1</sup>) and the first H<sub>2</sub>-transition (S<sub>0</sub>) from  $J = 0$  to  $J = 2$  appears at 354 cm<sup>-1</sup>. At increasing temperatures, the main fractional population of H<sub>2</sub> is thermally distributed above the ground-level rotational state that weakens the S<sub>0</sub> transition. However, in large proportions of H<sub>2</sub> at lower temperatures, the low-energy Lorentzian wing of the H<sub>2</sub> S<sub>0</sub>-line extends downward into the N<sub>2</sub> spectral envelope. This interference slightly up-converts the position of the N<sub>2</sub> spectral envelope and thereby it appears as if the temperature is increased. To eliminate such act, the H<sub>2</sub> S<sub>0</sub>-line was implemented in the code with molecular data reported in Herzberg<sup>24</sup> together with other spectroscopic essentials such as anisotropic polarizability<sup>25</sup> and Raman linewidth.<sup>26</sup> The implemented theory was calibrated by tuning the H<sub>2</sub> Raman cross section against measurements of N<sub>2</sub> and H<sub>2</sub> RCARS integrated signals for all the concentrations tested.

The method of modeling the N<sub>2</sub>  $J$ -dependent collisional broadening with differing binary mixtures of N<sub>2</sub> and H<sub>2</sub> is central to the current investigation. This was simulated using a Raman linewidth model implemented as a concentration weighted linear combination between the species-specific contributions according to

$$\Gamma_{J,J+2}^{N_2} = [N_2] \cdot \Gamma_{J,J+2}(N_2 - N_2) + [H_2] \cdot \Gamma_{J,J+2}(N_2 - H_2). \quad (2)$$

For comparison, three theoretical libraries were generated with the following sources of data: (1) measured time-domain coefficients (this study and Ref. 18); (2) the linewidths employed in Ref. 9 (N<sub>2</sub>-N<sub>2</sub> ECS and N<sub>2</sub>-H<sub>2</sub> ECS-EP); and (3) S-branch N<sub>2</sub>-H<sub>2</sub> broadening coefficients reported in Dhyne *et al.*<sup>27</sup> in combination with the measured N<sub>2</sub>-N<sub>2</sub> reported in Ref. 18. In order to be implemented for the contour spectral fitting procedure, the measured coefficients obtained at the specific oven temperatures needed to be transposed to intermediate temperatures evenly distributed within the boundaries of the given set. This was accomplished by applying bilinear interpolation to the experimental data distributed in two dimensions, maintaining the dependence on temperature as well as rotational quantum number.

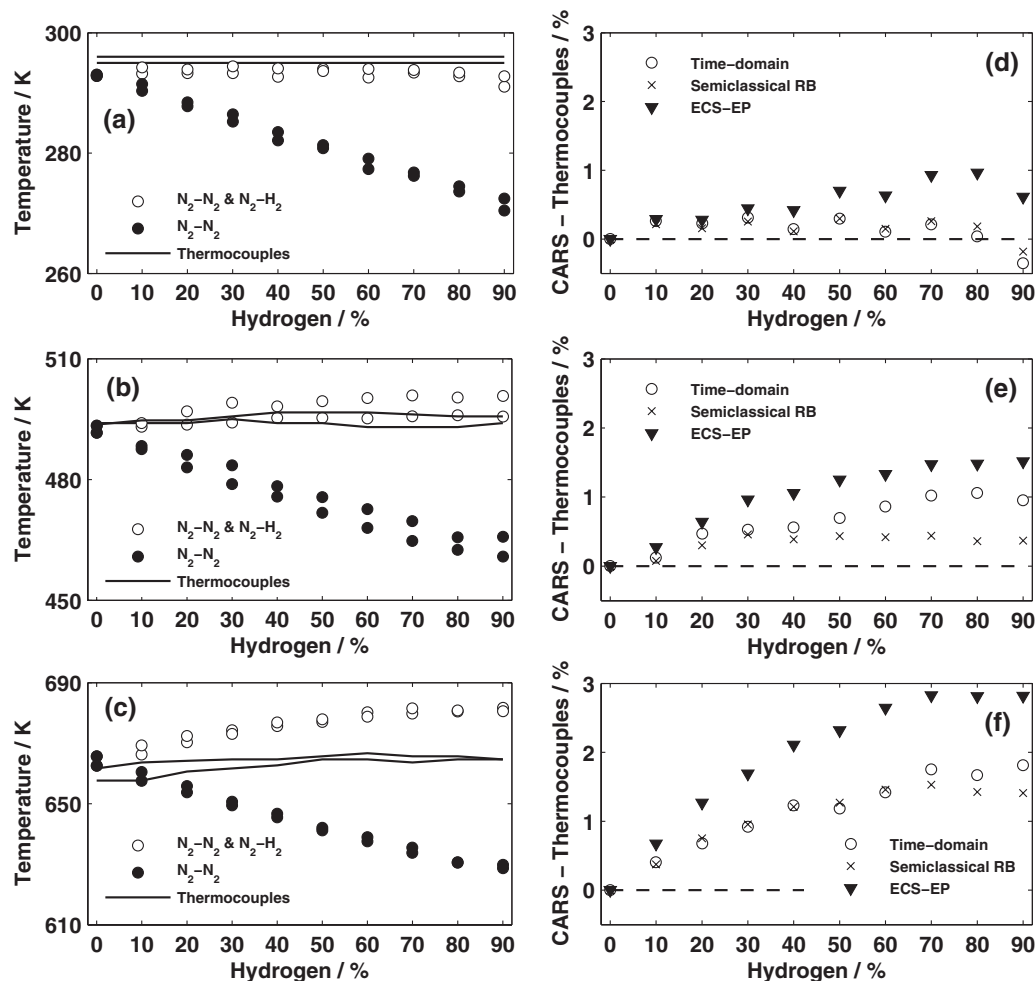


FIG. 4. (Left panels) Evaluated CARS temperatures using two different Raman linewidth models consisting of measured time-domain coefficients of either pure self-broadened  $N_2$  or a concentration weighted linear combination of both  $N_2-N_2$  and  $N_2-H_2$  at reference temperatures (a) 296 K, (b) 495 K, and (c) 661 K. (Right panels) Temperature difference between CARS and thermocouples, employing a Raman linewidth model according to Eq. (2) but applied with coefficients from different sources, time-domain picosecond CARS measurements, semi-classical RB calculations,<sup>27</sup> or a ECS-EP scaling law<sup>7</sup> at reference temperatures (d) 296 K, (e) 495 K, and (f) 661 K.

The experiments were performed at temperatures 296 K, 495 K, and 661 K in binary mixtures of  $N_2$  and  $H_2$  where the content of  $H_2$  was varied from 0%–90%, in steps of 10%. The gases were mixed using a flow meter controller (Definer 220, Bios), with each of the two species regulated as parts of a total flow of 2 l/min, resulting in an estimated uncertainty of the concentrations around 1%. The gas mixtures were heated in an inconel cylindrical cell (length 240 mm, diameter 28 mm) covered with standard heating tape (Hemi Heating AB, Sweden), and mounted with three thermocouples of type K (Pentronic AB, Sweden) for online calibration of the temperature. At each of the experimental conditions, 1000 single shots were collected and averaged for temperature evaluation.

The results are presented in Fig. 4, displayed in  $3 \times 2$  panels. In the panels on the left, CARS temperatures are shown with on-line monitored thermocouple temperatures, from two recorded experimental series at each of the three cases. In the data analysis method, the spectral fits are performed on averaged spectra. The relative standard deviations of single shot data, however, are the same for all the models employed and are about 4.5% for all the investigated temperatures. To contrast the evaluated temperatures obtained

with a Raman linewidth model according to Eq. (2), instead a theoretical library calculated with pure self-broadened  $N_2$  coefficients was used. This is to demonstrate the major underestimation in predicted temperature if the effects of  $N_2-H_2$  collisions on the spectra are neglected. It can be seen that the impact on thermometry is as much as 6% at hydrogen concentrations of 80%–90%, which is slightly less than obtained in the previous study.<sup>9</sup> By incorporating the complete model of Eq. (2), almost perfect agreement between CARS and thermocouple temperatures is reported at the reference cases, 296 K and 495 K, for all the binary mixtures, while at 661 K the predictions of the different approaches start to deviate slightly at increased concentration of  $H_2$ . It was discovered that by encapsulating the cell in a heat reservoir held at a constant temperature of 661 K and thereafter switching the gas inside the cell from  $N_2$  to  $H_2$  led to an increase in the thermocouple temperature reading of about 3 K. This temperature difference might be a consequence of  $H_2$  penetrating the inconel-mantling of the thermocouples, changing the thermochemical potential and thereby the temperature reading.

In panels on the right of Fig. 4, the difference in temperature between CARS and thermocouples are compared for the

different libraries applying the same Raman linewidth model (Eq. (2)) but combined with coefficients from the different sources. To isolate the impact on RCARS thermometry of implementing the various  $N_2$ - $H_2$  coefficients, the temperature difference between CARS and thermocouple-estimated temperatures at 100%  $N_2$  has been subtracted from all values. It should be noted that the case with pure  $N_2$  has recently been reported in a related study,<sup>18</sup> and it was found that by applying pure  $N_2$  self-broadening time-domain coefficients, the temperature uncertainty was less than 1%. In the current study, the spread in results between the different models is about 1%–1.5%. It can be seen that with the time-domain coefficients, the thermometry has been improved in comparison with the coefficients from previous work that attempted to account for the effect of  $H_2$ ,  $N_2$ - $N_2$  (Ref. 21) (ECS), and  $N_2$ - $H_2$ <sup>7</sup> (ECS-EP), and the performance with the newly calculated  $N_2$ - $H_2$  coefficients<sup>27</sup> is even slightly better. The estimated uncertainty for both these new sets, derived as the difference in percentage from the thermocouple reference temperature, is less than 2%.

#### IV. CONCLUSIONS

We have demonstrated the applicability of time-resolved picosecond RCARS in retrieving S-branch Raman linewidths of  $N_2$  perturbed by  $H_2$ . The measurements were performed at temperatures from 294 K to 1466 K and at each of the conditions the extracted line-broadening coefficients covered about 95% of the  $N_2$  rotational population distribution. This is an improvement from previous spectroscopic methods, where the experimental data have been provided at a more confined range of both temperatures as well as rotational quantum numbers. To quantify the validity of these coefficients for rotational CARS thermometry, they were incorporated in the analysis of  $N_2$  spectra recorded in binary mixtures with  $H_2$  heated up to 661 K. It was found that for all the conditions the set was within 2% in difference from the reference temperature. Hence, this is the expected accuracy for this technique when applied at the fuel-side of a hydrogen/air-diffusion flame, which resembles the conditions of this investigation.

This technique for acquiring *in situ* Raman linewidths may provide useful data to support the CARS community where there is a current lack of literature for various collision partners. In the nearest future, projects are planned to address S-branch  $N_2$  linewidths from other fuel molecules, such as methane, ethane, and propane.

#### ACKNOWLEDGMENTS

P.E.B., A.B., and E.N. acknowledge the financial support of the Swedish Energy Agency through the Center of Com-

bustion Science and Technology. Funding is also provided by the U.S. Department of Energy, Office of Basic Energy Sciences, Division of Chemical Sciences. Sandia is a multiprogram laboratory operated by Sandia Corporation, a Lockheed Martin Company, for the U.S. Department of Energy's National Nuclear Security Administration under Contract No. DE-AC04-94AL85000.

- <sup>1</sup>A. C. Eckbreth, *Laser Diagnostics for Combustion Temperature and Species* (Gordon and Breach, Amsterdam, 1996).
- <sup>2</sup>S. Roy, J. R. Gord, and A. K. Patnaik, *Prog. Energy Combust. Sci.* **36**, 280 (2010).
- <sup>3</sup>A. Bohlin and P.-E. Bengtsson, *Proc. Combust. Inst.* **33**, 823 (2011).
- <sup>4</sup>F. Vestin, M. Afzelius, C. Brackmann, and P.-E. Bengtsson, *Proc. Combust. Inst.* **30**, 1673 (2004).
- <sup>5</sup>L. Gomez, D. Bermejo, P. Joubert, and J. Bonamy, *Mol. Phys.* **104**, 1869 (2006).
- <sup>6</sup>L. Gomez, R. Z. Martinez, D. Bermejo, F. Thibault, B. Bussery-Honvault, P. Joubert, and J. Bonamy, *J. Chem. Phys.* **126**, 204302 (2007).
- <sup>7</sup>P. Joubert, J. Bonamy, L. Gomez, and D. Bermejo, *J. Raman Spectrosc.* **39**, 707 (2008).
- <sup>8</sup>A. Bohlin, F. Vestin, P. Joubert, J. Bonamy, and P.-E. Bengtsson, *J. Raman Spectrosc.* **40**, 788 (2009).
- <sup>9</sup>A. Bohlin, F. Vestin, P. Joubert, J. Bonamy, and P.-E. Bengtsson, *J. Raman Spectrosc.* **41**, 875 (2010).
- <sup>10</sup>G. Millot, *J. Chem. Phys.* **93**, 8001 (1990).
- <sup>11</sup>L. Bonamy, J. Bonamy, D. Robert, B. Lavorel, R. Saint-Loup, R. Chaux, J. Santos, and H. Berger, *J. Chem. Phys.* **89**, 5568 (1988).
- <sup>12</sup>L. Gomez, S. V. Ivanov, O. G. Buzykin, and F. Thibault, *J. Quant. Spectrosc. Radiat. Transf.* **112**, 1942 (2011).
- <sup>13</sup>T. Seeger, J. Kiefer, A. Leipertz, B. D. Patterson, C. J. Klierer, and T. B. Settersten, *Opt. Lett.* **34**, 3755 (2009).
- <sup>14</sup>T. Seeger, J. Kiefer, Y. Gao, B. D. Patterson, C. J. Klierer, and T. B. Settersten, *Opt. Lett.* **35**, 2040 (2010).
- <sup>15</sup>C. J. Klierer, Y. Gao, T. Seeger, J. Kiefer, B. D. Patterson, and T. B. Settersten, *Proc. Combust. Inst.* **33**, 831 (2011).
- <sup>16</sup>C. J. Klierer, Y. Gao, T. Seeger, B. D. Patterson, R. L. Farrow, and T. B. Settersten, *Appl. Opt.* **50**, 1770 (2011).
- <sup>17</sup>M. Schenk, T. Seeger, and A. Leipertz, *Appl. Opt.* **39**, 6918 (2000).
- <sup>18</sup>C. J. Klierer, A. Bohlin, E. Nordström, B. D. Patterson, P.-E. Bengtsson, and T. B. Settersten, "Time-domain measurements of S-branch  $N_2$ - $N_2$  Raman linewidths using picosecond pure rotational coherent anti-Stokes Raman spectroscopy," *Appl. Phys. B*, doi:10.1007/s00340-012-5037-2 (in press).
- <sup>19</sup>A. E. Depristo, S. D. Augustin, R. Ramaswamy, and H. Rabitz, *J. Chem. Phys.* **71**, 850 (1979).
- <sup>20</sup>M. L. Koszykowski, L. A. Rahn, R. E. Palmer, and M. E. Coltrin, *J. Phys. Chem.* **91**, 41 (1987).
- <sup>21</sup>L. Martinsson, P.-E. Bengtsson, M. Aldén, S. Kröll, and J. Bonamy, *J. Chem. Phys.* **99**, 2466 (1993).
- <sup>22</sup>A. Bohlin, P.-E. Bengtsson, and M. Marrocco, *J. Raman Spectrosc.* **42**, 1843 (2011).
- <sup>23</sup>R. H. Tipping and J. F. Ogilvie, *J. Raman Spectrosc.* **15**, 38 (1984).
- <sup>24</sup>G. Herzberg, *Molecular Spectra and Molecular Structure* (Robert E. Krieger Publishing Company, Florida, 1989), Vol. I.
- <sup>25</sup>C. Asawaroengchai and G. M. Rosenblatt, *J. Chem. Phys.* **72**, 2664 (1980).
- <sup>26</sup>H. G. M. Edwards, D. A. Long, and G. Sherwood, *J. Raman Spectrosc.* **22**, 607 (1991).
- <sup>27</sup>M. Dhyne, M. Lepère, and P. Joubert, "Semiclassical line broadening calculations, using an *ab initio* potential energy surface, in Q-branch and S-branch of  $N_2$  perturbed by  $H_2$ ," *J. Raman Spectrosc.* (in press).